Conformation and Dynamics of Melittin Bound to Magnetically Oriented Lipid Bilayers by Solid-State ^{31}P and ^{13}C NMR Spectroscopy

Akira Naito, Takashi Nagao, Kazushi Norisada, Takashi Mizuno, Satoru Tuzi, and Hazime Saitô
Department of Life Science, Faculty of Science, Himeji Institute of Technology, Harima Science Garden City, Hyogo 678-1297, Japan

ABSTRACT The conformation and dynamics of melittin bound to the dimyristoylphosphatidylcholine (DMPC) bilayer and the magnetic orientation in the lipid bilayer systems were investigated by solid-state ^{31}P and ^{13}C NMR spectroscopy. Using ^{31}P NMR, it was found that melittin-lipid bilayers form magnetically oriented elongated vesicles with the long axis parallel to the magnetic field above the liquid crystalline-gel phase transition temperature (T_m = 24°C). The conformation, orientation, and dynamics of melittin bound to the membrane were further determined by using this magnetically oriented lipid bilayer system. For this purpose, the ^{13}C NMR spectra of site-specifically ^{13}C-labeled melittin bound to the membrane in the static, fast magic angle spinning (MAS) and slow MAS conditions were measured. Subsequently, we analyzed the ^{13}C chemical shift tensors of carbonyl carbons in the peptide backbone under the conditions where they form an α-helix and reorient rapidly about the average helical axis. Finally, it was found that melittin adopts a transmembrane α-helix whose average axis is parallel to the bilayer normal. The kink angle between the N- and C-terminal helical rods of melittin in the lipid bilayer is ~140° or ~160°, which is larger than the value of 120° determined by x-ray diffraction studies. Pore formation was clearly observed below the T_m in the initial stage of lysis by microscope. This is considered to be caused by the association of melittin molecules in the lipid bilayer.

INTRODUCTION

Melittin is a hexacosapeptide with a primary structure of Gly-Ile-Gly-Ala-Val-Leu-Lys-Val-Leu-Thr-Thr-Gly-Leu-Pro-Ala-Leu-Ile-Ser-Trp-Ile-Lys-Arg-Lys-Arg-Gln-Gln-NH_2 and is a main component of bee venom (Habermann and Jentsch, 1967). Melittin is monomeric, with a disordered conformation in dilute aqueous solution (Talbot et al., 1979; Lauterwein et al., 1980) and an α-helix in methanol (Bazzo et al., 1988). In contrast, melittin is a tetramer with a helical structure in high ionic strength and high pH in an aqueous solution (Brown et al., 1980). In the crystalline state, a single polypeptide chain of melittin consists of two α-helical rods, residues 1–10 and 13–26, making a kink angle of ~120°, and forms a tetrameric complex, as revealed by x-ray diffraction studies at a resolution of 2 Å (Terwilliger et al., 1982; Terwilliger and Eisenberg, 1982).

Melittin has powerful hemolytic activity (Sessa et al., 1969) in addition to voltage-dependent ion conductance across planar lipid bilayers at low concentration (Tosteson and Tosteson, 1981; Kemf et al., 1982). It also causes selective micellization of bilayers as well as membrane fusion at high concentration (Habermann, 1972; Morgan et al., 1983). A number of studies have been performed to determine the nature of the interaction of melittin with membranes, although there is still no consensus on the nature of its interaction with membrane lipids, partly because many of the biophysical techniques applied to the study of protein structure and interaction are difficult to apply to membrane systems (Dempsey, 1990). From a structural point of view, orientation of the melittin helix in lipid bilayers is still controversial, although melittin is bound to membranes or detergent micelles, with a highly α-helical conformation (Dawson et al., 1978; Inagaki et al., 1989; Okada et al., 1994). Polarized infrared (Vogel et al., 1983) and attenuated total reflection Fourier transform infrared spectroscopy (ATR-FTIR) (Brauner et al., 1987) studies showed that melittin was preferentially oriented parallel to the fatty acyl chains of lipids. ^{13}C NMR analysis of ^{13}C-labeled melittin in the oriented membrane on a glass plate showed that the peptide is oriented parallel to the bilayer normal (Smith et al., 1994). In contrast, the helical segments were preferentially oriented parallel to the bilayer plane by polarized attenuated total internal reflection-Fourier transform infrared spectroscopy (PATIR-FTIR) (Citra and Axelson, 1996). Accessibility measurements of spin-labeled melittin by chromium oxalate (Altenbach et al., 1989) and ^{13}C NMR in the presence of aqueous shift reagents (Stanislawski and Ruterjans, 1987) indicated the location of melittin on the membrane surface, with only the hydrophobic residues buried in the lipid bilayer. Later, ATR-IR study showed that the α-helix of melittin is oriented parallel and perpendicular to the bilayer surface in hydrated single planar bilayers and dry phospholipid multibilayers, respectively, depending on the condition of hydration (Frey and Tamm, 1991).

At a moderately high concentration, melittin is known to cause the breakdown of the lipid bilayer into micelles in a manner similar to that of solubilization by detergent (Habermann, 1972). This phenomenon has been extensively studied by means of light scattering, freeze-fracture electron

Received for publication 4 October 1999 and in final form 31 January 2000.

Address reprint requests to Dr. Akira Naito, Department of Life Science, Faculty of Science, Himeji Institute of Technology, Harima Science Garden City, Kamigori-cho, Hyogo, Japan 678-1297. Tel.: +81-791-58-0180; Fax: +81-791-58-0182; E-mail: naito@sci.himeji-tech.ac.jp.

0006-3495/00/05/2405/13 $2.00

microscopy, and nuclear magnetic resonance spectroscopy to understand the nature of the interaction of melittin with lipid bilayers (Dufourc et al., 1986a,b; Dempsey and Sternberg, 1991; Dufourcq et al., 1986; Dempsey and Watts, 1987). At a temperature above the liquid crystalline-to-gel phase transition temperature (T_m), lipid bilayers composed of saturated phosphatidylcholine are stable as extended vesicles. As the temperature is lowered to the gel phase, the lipid bilayer breaks down into small particles. As the temperature is raised back above the T_m, the extended bilayer reforms. Phase-dependent lysis and fusion are readily observable by ^{31}P and ^{2}H NMR spectroscopy (Dufourc et al., 1986; Dempsey and Watts, 1987). These authors proposed that the bilayer disc is formed below the T_m and surrounded by a belt of melittin molecules (Dufourcq et al., 1986). The presence of negatively charged lipids reduced the proportion of lysed vesicles (Monette and Lafleur, 1995), although melittin strongly binds negatively charged lipids with the electrostatic effect (Beschraschvili and Seelig, 1990).

One of the interesting properties of lipid bilayers containing melittin is their ability to magnetically orient in the presence of a strong magnetic field (Dempsey and Sternberg, 1991; Dempsey and Watts, 1987; Pott and Dufourc, 1995). Similar orientation effects have been reported in pure and mixed phospholipid bilayer systems (Scholz et al., 1984; Seelig et al., 1985; Speyen at al., 1987; Brumm et al., 1992; Qiu et al., 1993). Actually, the long axis of the elongated vesicle is aligned parallel to the magnetic field, owing to the presence of a large diamagnetic susceptibility $\Delta\chi$. Recently, a disc-type bilayer system, a bicelle, has been reported to show magnetic ordering in which the bilayer surface is aligned parallel to the magnetic field (Sanders and Prestegard, 1990; Sanders and Schwonek, 1992). This bicelle system is used to elucidate the structure of membrane proteins after they are reconstituted into bicelles (Howard and Opella, 1996).

It is therefore expected that the manner of orientation of melittin bound to the lipid bilayer can be directly determined by observing the ^{13}C NMR signals of ^{13}C-labeled melittin, because the axis of orientation of the lipid bilayer in the magnetic field is now well characterized. In particular, it is very important to determine how melittin molecules are oriented in highly hydrated lipid bilayers under physiological conditions. Therefore we attempted here to use this magnetic orientation of a lipid bilayer containing melittin to investigate the structure, orientation, and dynamics of melittin bound to the magnetically oriented lipid bilayer to understand the interactions of melittin with membranes.

MATERIALS AND METHODS

Sample preparation

Five selectively ^{13}C-labeled melittins, [1-^{13}C]Gly^{3}, [3-^{13}C]Ala^{15} doubly labeled (I), and [1-^{13}C]Val^{5}, [1-^{13}C]Gly^{12}, [1-^{13}C]Leu^{16}, or [1-^{13}C]Ile^{20} singly labeled melittins (II–V), were synthesized, using an Applied Biosystems 431A peptide synthesizer, by means of a solid-phase method (Fields et al., 1992). 9-Fluorenylmethoxycarbonyl (Fmoc)-labeled amino acids were synthesized from 9-fluorenyl *N*-succinimidyl carbonate (Fmoc Osu) and isotopically labeled amino acids, following a method by Paquet (1982). Synthesized peptides were purified using a Waters 600E high-performance liquid chromatography system with a Bondasphere C_{18} reversed-phase column. Fifty milligrams of melittin and dimyristoylphosphatidylcholine (DMPC), with a melittin-to-DMPC molar ratio of 1:10, was dissolved in chloroform, and the solvent was subsequently evaporated in vacuo, followed by hydration with 900 μl of deionized water or Tris buffer (20 mM Tris, 100 mM NaCl, and pH 7.5). A freeze-thaw cycle was repeated 10 times, followed by centrifugation to concentrate the bilayers at 27°C. This process was repeated three times, and finally the total volume was adjusted to 300 μl containing 50 mg of lipid and melittin. This indicates that the water content was ~80% (w/w). The lipid bilayers were filled in zirconia or glass sample tubes and sealed with glue to prevent dehydration.

NMR measurements

^{13}C and ^{31}P NMR spectra were recorded on a Chemagnetics CMX-400 NMR spectrometer at the ^{13}C and ^{31}P resonance frequencies of 100.64 and 161.98 MHz, respectively, under static or magic angle spinning (MAS) conditions. NMR spectra were measured using 5 μs of 90° excitation pulse followed by acquisition of signals under the high power proton decoupling rf pulse of 50 kHz. In the ^{31}P NMR measurements, 200 transients were accumulated with a repetition time of 2 s. In the ^{13}C NMR measurements, 8000–10,000 transients were accumulated with a repetition time of 5 s. A cross-polarization experiment with a contact time of 1 ms was performed only at −60°C, because it was not efficient in a temperature range from 10 to 40°C. In the MAS experiment, spinning frequencies were adjusted to 3000 ± 3 and 100 ± 10 Hz for the fast and slow MAS experiments, respectively. Lorentzian line broadening of 30 and 20 Hz was applied before Fourier transformation for the static and MAS experiments, respectively. ^{31}P and ^{13}C chemical shift values were referred to those of 85% H_3PO_4 and tetramethylsilane (TMS) after conversion from 176.03 ppm of the carboxyl carbon of glycine as external references, respectively. NMR measurements were started after a wait of 30 min to equilibrate the temperature of the lipid bilayer systems. The temperatures of samples in the static and MAS experiments were monitored with a thermocouple attached to the inlet of the probe head.

Microscopic measurements

Microscope pictures were obtained with a Carl Zeiss Axiophot microscope in differential-interference mode. The temperature of the bilayer dispersion prepared as described above was controlled in a temperature range from 5 to 40°C, using a temperature-controlled stage for the microscope (Tokai Hit, Shizuoka, Japan). A nitrogen gas stream was applied for a low-temperature experiment to prevent vapor condensation. The same lipid bilayer sample used for the NMR measurements was diluted five times with Tris buffer, and 40 μl of the sample was placed on a glass plate and covered by a thin glass plate. The edge of the cover glass was sealed with clear nail polish to prevent dehydration.

RESULTS

Orientation of DMPC bilayers containing melittin to the magnetic field

Fig. 1 shows ^{31}P NMR spectra recorded at a variety of temperatures for melittin-DMPC bilayers hydrated with

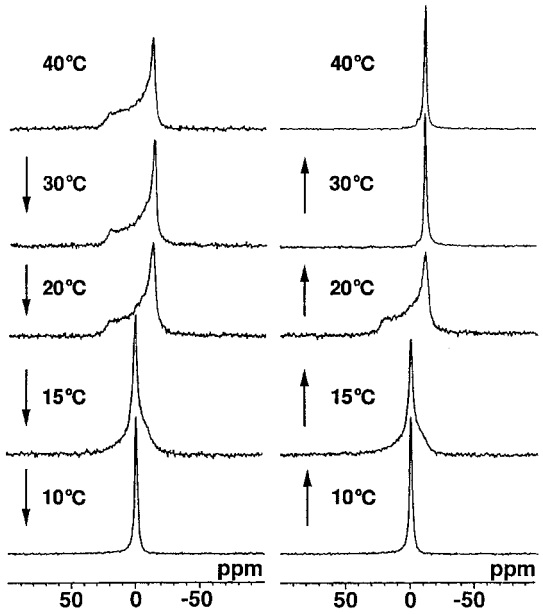

FIGURE 1 Temperature variation of ^{31}P NMR spectra of melittin-DMPC bilayers hydrated with deionized water. The arrows indicate the process of temperature changes.

deionized water. Immediately after the sample was placed in the magnetic field, the ^{31}P NMR spectra were recorded at 40°C. An axially symmetrical powder pattern characteristic of the liquid crystalline phase was observed at 40°C. When the temperature was lowered to 30°C, the intensity of the right edge of the powder pattern (perpendicular component) was increased. At 15°C, an isotropic component caused by lysis in the presence of melittin appeared near 0 ppm, and it dominated at 10°C. When the temperature was raised from 10°C, the same anisotropic powder patterns as a result of fusion were obtained up to 20°C. At a temperature higher than 30°C, a single line was observed at −12 ppm, corresponding to the perpendicular component of the ^{31}P chemical shift tensor of the liquid crystalline bilayer (Smith and Ekiel, 1984). This result indicates that the lipid bilayer surface is oriented parallel to the magnetic field (Dempsey and Sternberg, 1991; Dempsey and Watts, 1987) at a temperature higher than 30°C, although it is not magnetically aligned before the temperature is lowered. It should be emphasized that once lysis was completed and the temperature was raised again to fuse the lipid bilayer in the magnetic field, highly ordered alignment to the magnetic field is achieved. We also noticed that the magnetic ordering disappeared at 20°C, which is slightly lower than the liquid crystal-to-gel transition temperature (T_m = 24°C) of the pure DMPC bilayer. The relative change of order parameter of the melittin-DMPC bilayer with respect to the pure DMPC bilayer, $S_{bilayer}$ (Sanders, 1993), was determined to be 0.76 from the perpendicular component ($\delta_\perp$ = −15.8 ppm) of the powder pattern in the pure DMPC bilayer prepared under the same conditions as the melittin-DMPC bilayer.

When the temperature was raised from 20°C to 30°C, it took on the order of minutes to show a sharp line at −12 ppm, indicating the magnetic ordering (Fig. 2 *a*). Because the rate of magnetic ordering in the magnetic field is not fast, one can expect to obtain a powder pattern when the slow magic angle spinning experiment is performed. Actually, an axially symmetrical powder pattern was observed when the spinning frequency of 100 Hz was applied as shown in Fig. 2 *b*. This fact indicates that magnetic ordering can be disturbed by a slow MAS experiment. In this work, the slow spinning frequency of 100 Hz is chosen, which is fast enough to disturb the magnetic orientation but slow enough to give sideband free powder patterns. The observation of the powder pattern in the slow MAS experiment is useful for obtaining information on the structure and dynamics of melittin bound to membranes, as is described later.

Microscopic observation of the lytic process in melittin-DMPC bilayer systems

Fig. 3 shows the microscopic picture of melittin-DMPC bilayer systems. Giant vesicles with a diameter larger than 20 μm were observed after the melittin-DMPC dispersion was kept at 25°C for 3 h. Vesicle fusion was clearly seen at the center region of the top figure. When the temperature was lowered to 15°C, a number of pores appeared at the surface of vesicles, which results in the breakdown of vesicles. Consequently, the vesicles disappeared completely at 10°C. When the temperature was raised back to 25°C, small

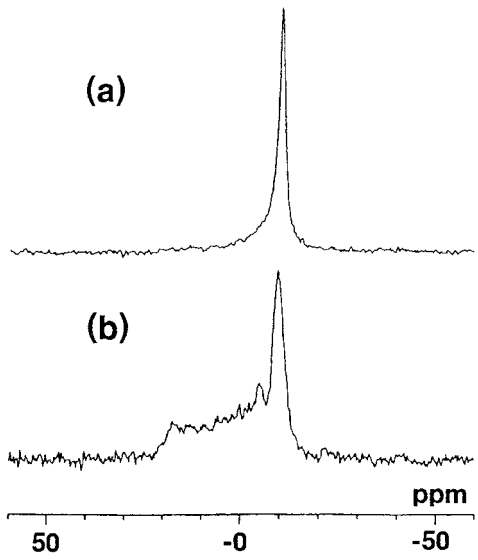

FIGURE 2 ^{31}P NMR spectra of melittin-DMPC bilayers in static (*a*) and slow MAS (spinning frequency of 100 Hz) (*b*) conditions.

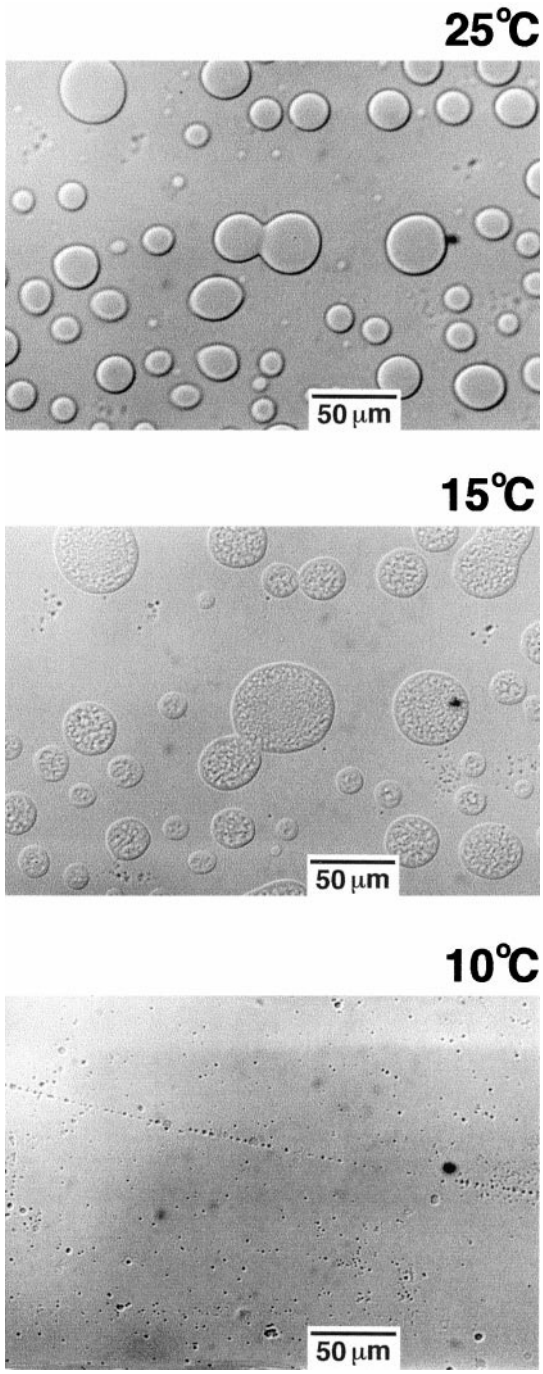

FIGURE 3 Differential-interference microscopic pictures of melittin-DMPC bilayers hydrated with Tris buffer, taken at 25, 15, and 10°C.

spherical vesicles with a diameter of ~5 μm appeared after 10 min and fused with each other, growing into larger vesicles. Therefore, lysis and fusion occurred reversibly at around T_m (24°C). It is therefore expected that when this fusion process occurs in the magnetic field, elongated vesicles are formed, as is observed in the ^{31}P NMR spectra of melittin-DMPC bilayer systems.

^{13}C NMR spectra of melittin-DMPC bilayer systems

Fig. 4 shows the ^{13}C NMR spectra of [1-^{13}C]Gly^3, [3-^{13}C]Ala^{15} doubly labeled melittin (I) in DMPC hydrated with deionized water. The temperature was raised from 10°C to ensure that the bilayer is magnetically oriented at a temperature higher than 30°C. The ^{13}C NMR signals of melittin that resonated at 173.2 and 15.8 ppm at 10°C were assigned to Gly^3 C═O and Ala^{15} CH_3 carbon nuclei, respectively, by subtracting the signals of lipid bilayers containing unlabeled melittin from the signals of bilayers containing labeled melittin, as shown in Fig. 4 *f*. ^{13}C NMR signals from melittin and DMPC were broadened at 20°C, when the lipid bilayer was not magnetically oriented as shown in the ^{31}P NMR spectra (Fig. 1). This result indicates that melittin interacts strongly with the lipid bilayer. At

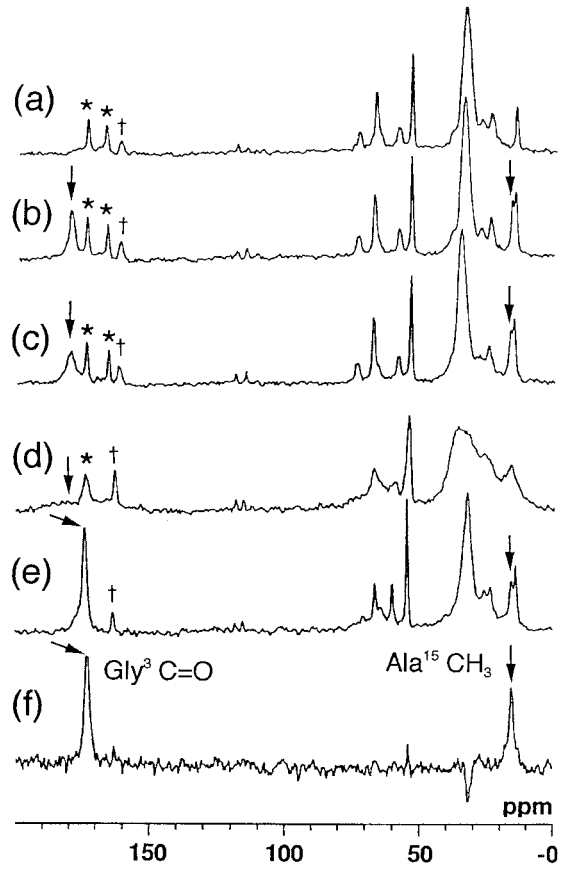

FIGURE 4 Temperature variation of ^{13}C NMR spectra of DMPC bilayers in the presence of [1-^{13}C]Gly^3, [3-^{13}C]Ala^{15}-melittin in the static condition. The ^{13}C chemical shifts values were referred to TMS. (*a*) Unlabeled melittin-DMPC systems at 40°C. (*b–e*) Labeled melittin-DMPC bilayer system at 40°C (*b*), 30°C (*c*), 20°C (*d*), and 10°C (*e*). (*f*) Difference spectrum between the labeled and unlabeled melittin-DMPC systems at 10°C. The arrowed peaks around 173–179 and 15–16 ppm indicate the ^{13}C NMR signals of Gly^3 ^{13}C═O and Ala^{15} $^{13}CH_3$, respectively. The signals marked by stars indicate the C═O groups of DMPC (Sanders, 1993). Unknown impurities in melittin are marked by daggers.

30°C, narrowing of the signal (linewidth is 620 Hz) for Gly^3 C═O of melittin started, and a narrower line (linewidth is 340 Hz) was recorded at 40°C, indicating that the motional frequency of the α-helical axis is much higher than 15 kHz, showing less interference with chemical shift broadening due to 15 kHz of anisotropy. The peak position at 40°C was displaced to 179.5 ppm, which is downfield by 6.3 ppm from the isotropic chemical shift value obtained at 10°C. In the magnetically oriented lipid bilayers at a temperature higher than 30°C, a new signal appeared at 166.5 ppm, which has been assigned to one of the C═O groups of the magnetically oriented membrane (Sanders, 1993). This result clearly indicates that melittin, as well as the lipid bilayer, is oriented in the magnetic field. Although a small signal due to impurity in melittin (marked by a dagger) was persistent despite purification by high-performance liquid chromatography, this impurity did not affect the behavior of the ^{13}C NMR spectra. We have also prepared the lipid bilayers with the Tris buffer, and similar results were observed (spectra not shown). (Tris buffer was used instead of deionized water for the sake of the longer stability of bilayers essential for ^{13}C NMR measurements for determining ^{13}C chemical shift values.) Similarly, the ^{13}C NMR signal of the methyl carbon of Ala^{15} was broadened at 20°C. In the oriented bilayer at 40°C, the signal was displaced to 17.2 ppm, which is 1.1 ppm downfield from the isotropic value. These displacements of the signal positions clearly indicate that melittin interacts with the bilayer, as viewed from the Ala^{15} and Gly^3 positions.

Fig. 5 shows the ^{13}C NMR spectra of [1-^{13}C]Ile^{20}-melittin bound to the DMPC bilayer hydrated with Tris buffer. A broad asymmetrical powder pattern characterized by δ_{11} = 241, δ_{22} = 189, and δ_{33} = 96 ppm appeared at −60°C (Fig. 5 *a*). The presence of this broad signal indicates that any motion of melittin bound to the DMPC bilayer is completely frozen at −60°C. A narrowed ^{13}C NMR signal was observed at 174.8 ppm for Ile^{20} C═O by fast MAS experiment at 40°C (Fig. 5 *d*), and its position was displaced upfield by 4.6 ppm in the oriented bilayer at 40°C, as observed in the magnetically oriented state (Fig. 5 *c*). An axially symmetrical powder pattern with an anisotropy of 14.9 ppm was recorded at 40°C in the slow MAS experiment (Fig. 5 *b*). Because the linewidth due to the anisotropy at 40°C is not as broad as that at −60°, it is expected that the α-helical segment undergoes rapid reorientation about the helical axis at 40°C.

^{13}C NMR spectra of a variety of ^{13}C-labeled melittins bound to the DMPC bilayer hydrated with Tris buffer at 40°C were compared among the samples of different ^{13}C labeling under the conditions of the magnetically oriented and fast MAS experiments (*arrowed peaks*), as shown in Fig. 6. The ^{13}C chemical shifts and linewidths thus obtained are summarized in Table 1, together with the anisotropies evaluated from the slow MAS ^{13}C NMR spectra and from the spectra obtained at −60°C (spectra not shown). It was

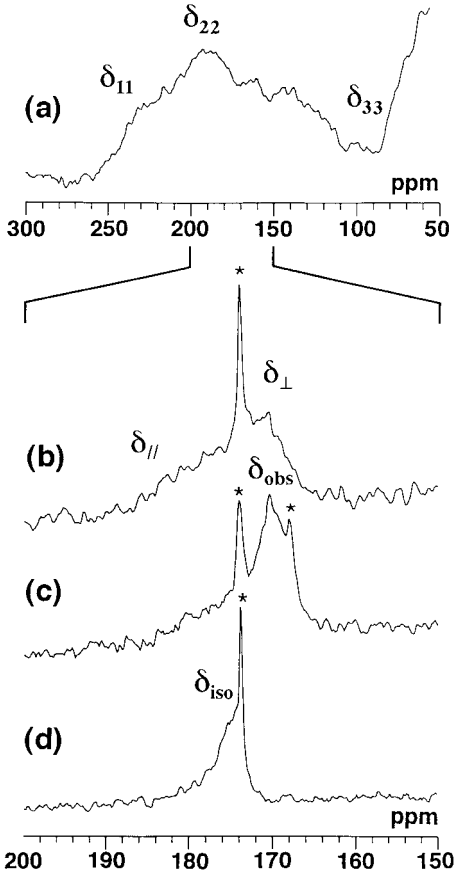

FIGURE 5 Temperature variation of ^{13}C NMR spectra of a DMPC bilayer in the presence of [1-^{13}C]Ile^{20}-melittin in the static condition at −60°C (*a*) and slow MAS (*b*), static (*c*), and fast MAS (*d*) conditions at 40°C. The signals (marked by *asterisks*) appearing at 173 ppm in *b*, 173 and 168 ppm in *c*, and 173 ppm in *d* are assigned to the C═O groups of DMPC.

observed that the ^{13}C NMR signal of Gly^3 C═O in the magnetically oriented state is displaced substantially downfield from that of the fast MAS experiment (superimposed on the signals from DMPC shown with an *asterisk*) by 6.8 ppm, whereas that of Gly^{12} C═O in the magnetically oriented state is displaced slightly upfield by 0.7 ppm from that in the fast MAS experiment. On the other hand, the ^{13}C chemical shift of [1-^{13}C]Ile^{20}-melittin in the magnetically oriented state is displaced upfield by 4.6 ppm from that of the fast MAS experiment.

^{13}C NMR spectra of the [1-^{13}C]amino acid-labeled melittin in DMPC bilayers recorded under the slow MAS condition were shown in Fig. 7. Note that the anisotropy $|\delta_{\|} - \delta_{\perp}|$ of [1-^{13}C]Gly^3-melittin is much larger than that of [1-^{13}C]Gly^{12}-melittin in the slow MAS experiment. In the axially symmetrical powder pattern for Gly^3, $\delta_{\perp}$ appeared at lower field than $\delta_{\|}$. In contrast, $\delta_{\perp}$ in the axially symmetrical pattern for the [1-^{13}C]Ile^{20}-melittin appeared at higher field than $\delta_{\|}$, and the anisotropy was again much larger than that of [1-^{13}C]Gly^{12}-melittin. Anisotropies $|\delta_{\|} - \delta_{\perp}|$ for [1-^{13}C]Val^5-melittin and

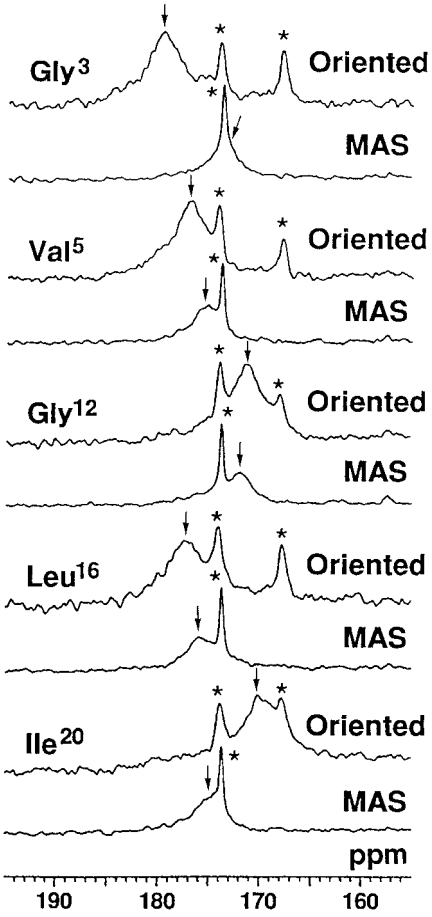

FIGURE 6 ^{13}C NMR spectra of carbonyl carbons for a variety of ^{13}C-labeled melittin bound to DMPC bilayers in the static (magnetically oriented) and MAS conditions, as indicated by the arrows. The signals marked by asterisks indicate the C═O groups of DMPC.

[1-^{13}C]Leu^{16}-melittin were also observed to be very small. The observed isotropic chemical shifts for these labeled portions (Table 1) indicate that all of these labeled moieties of melittin are involved in the α-helical structure with reference to those of the conformation-dependent ^{13}C chemical shifts of model systems (Saitô and Ando, 1989; Saitô et al., 1998). Because these isotropic chemical shifts did not vary at $-60°C$ as summarized in Table 1, the α-helical conformation persists in the lysed state. As discussed later, these chemical shift values of the magnetically aligned state also provide information on the orientation of the melittin helix with respect to the surface of the lipid bilayer.

DISCUSSION

Mechanism of magnetic ordering of the lipid bilayer containing melittin

Magnetic ordering of lipid bilayers has been reported for pure (Qiu et al., 1993) and mixed (Scholz et al., 1984; Seelig et al., 1985; Speyen et al., 1987; Brumm et al., 1992) phosphatidylcholine bilayers, including melittin-phospholipid systems (Dempsey and Sternberg, 1991; Dempsey and Watts, 1987; Pott and Dufourc, 1995). Subsequently, such magnetic ordering has been reported in a detergent/lipid mixture called a bicelle (Sanders and Prestegard, 1990; Sanders and Schwonek, 1992; Sanders, 1993), which was shown to be oriented in the magnetic field by the negative magnetic anisotropy of the lipid acyl chain. Therefore, the acyl chain tends to orient perpendicular to the magnetic field if a large number of lipid molecules are ordered in the liquid crystalline phase to possess a sufficient degree of magnetic anisotropy to align lipid bilayers along the magnetic field. Recently, orientation of the magnetic ordering was shown to be flipped by 90° by the addition of lanthanide ions such as Eu^{3+}, which have positive magnetic anisotropy (Prosser et al., 1996). Therefore, the magnetic ordering of DMPC bilayers containing melittin can be explained in terms of the morphology of the lipid bilayers. It has been reported that discoidal bilayers are formed in the presence of melittin surrounding them at a temperature lower than the T_m, and they re-fuse to form a large bilayer at a temperature higher than T_m (Dufourcq et al., 1986). Morphologically, this disc should be very similar to the bicelle.

In this study, ^{31}P NMR spectra and microscopic observation clearly show that in the moderately high concentration of melittin incorporated into the DMPC bilayer (DMPC/melittin = 10:1 molar ratio), the bilayer shows lysis and fusion at temperatures lower and higher than the T_m, respectively, which is consistent with the finding by Dufourc et al. (1986). It was also reported that unilameller vesicles are formed at a temperature higher than the T_m as a result of fusion (Dufourcq et al., 1986). Indeed, giant vesicles were observed above the T_m in this work by microscope for this melittin-DMPC bilayer system. We also noticed that the magnetic ordering occurs at a temperature higher than the T_m. Therefore, it is suggested that elongated bilayer vesicles rather than discoidal bilayers are formed above the T_m in the case of the melittin-DMPC bilayer system, in which most of the surface area of the bilayers is oriented parallel to the magnetic field, as shown schematically in Fig. 8. Thus a large magnetic anisotropy can be induced because most of the phospholipids, which have negative magnetic anisotropy along the acyl chain axes, are aligned perpendicular to the magnetic field. Similar elongated vesicles have been reported in the case of phospholipid mixtures (Scholz et al., 1984; Seelig et al., 1985; Speyer et al., 1987; Brumm et al., 1992) and the dynorphin-DMPC bilayer system (Naito et al., manuscript in preparation). It should be emphasized that the DMPC bilayer containing melittin shows highly magnetic ordering because an almost pure perpendicular component of ^{31}P NMR signals was seen, as shown in Figs. 1 and 2, provided that the bilayer system passed once through the lysed state. This

TABLE 1 ^{13}C chemical shift values (ppm) and structure and orientation of melittin bound to magnetically oriented lipid bilayers at 40°C

	δ_{obs}	$\Delta\delta_{obs}$*	δ_{iso}	$\Delta\delta_{iso}$*	$\delta_{\parallel} - \delta_{\perp}$	δ_{11}†	δ_{22}†	δ_{33}†	Structure‡	θ§
[1-^{13}C]Gly^{3}	179.5 ± 0.2	3.4	172.7 ± 0.2 (172.4)‡	2.4	−20.7 ± 2.0	237.6	186.7	92.9	α-helix	86° ± 10°
[1-^{13}C]Val^{5}	177.0 ± 0.2	3.6	175.2 ± 0.2 (175.2)‡	3.4	−5.4 ± 0.8	237.6	191.1	96.9	α-helix	90° ± 15°
[1-^{13}C]Gly^{12}	170.9 ± 0.3	4.1	171.6 ± 0.2 (171.6)‡	3.2	~0	240.6	180.7	93.5	α-helix	—
[3-^{13}C]Ala^{15}	17.2 ± 0.1	1.4	16.1 ± 0.1 (15.8)‡	1.4	—				α-helix	—
[1-^{13}C]Leu^{16}	177.2 ± 0.3	4.2	175.6 ± 0.2 (175.5)‡	3.2	−6.2 ± 1.0	240.6	192.8	93.1	α-helix	74° ± 15°
[1-^{13}C]Ile^{20}	170.2 ± 0.3	4.3	174.8 ± 0.2 (175.1)‡	3.4	14.9 ± 2.0	240.6	188.9	96.1	α-helix	81° ± 10°

*Linewidth at the half-height.

†Obtained at −60°C and the error range for the tensor elements are ±1.5 ppm.

‡Typical ^{13}C chemical shift values (ppm) of (δ_{iso} of α-helix, δ_{iso} of β-sheet) are (171.6, 168.5), (174.9, 171.8), (15.5, 20.3), (175.7, 170.5), and (174.9, 172.7) for Gly C═O, Val C═O, Ala CH_3, Leu C═O, and Ile C═O, respectively (Saitô and Ando, 1989).

§θ values indicate the angles between the average helical axis and the membrane surface.

unusually long elongated vesicle can be formed in the presence of a strong magnetic field because the elongated vesicle is considered to be stabilized by melittin molecules, particularly in the presence of a magnetic field. It is not likely, however, that the α-helix of melittin itself in the lipid bilayer plays an essential role in aligning the lipid bilayer, although an α-helix has positive diamagnetic anisotropy along the helical axis because of the axial alignment of the peptide bonds (Worcester, 1978). This is because the α-helix of melittin is aligned perpendicular to the bilayer surface, as discussed later.

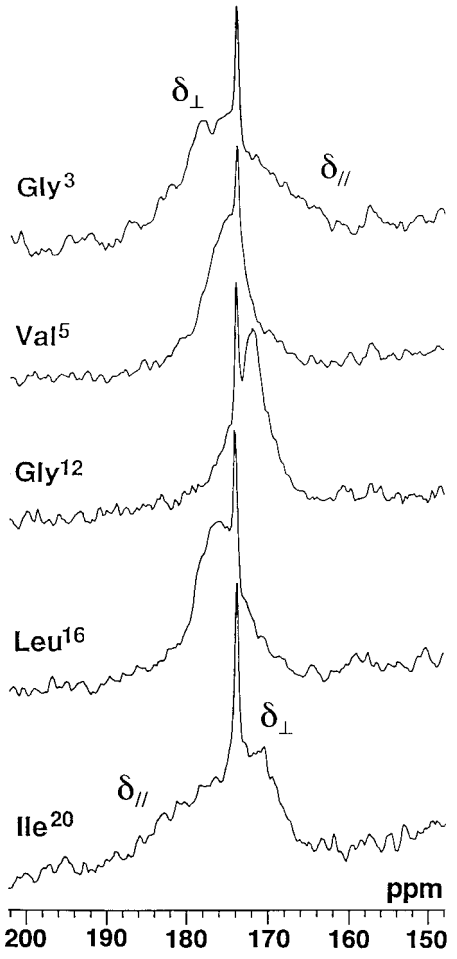

FIGURE 7 ^{13}C NMR spectra of carbonyl carbons for a variety of ^{13}C-labeled melittin bound to DMPC bilayers in the slow MAS condition. The sharp signals at 174 ppm indicate the C═O groups of DMPC.

Conformation of melittin bound to DMPC bilayers

The secondary structure of melittin bound to DMPC bilayers can be determined in an empirical manner by utilizing

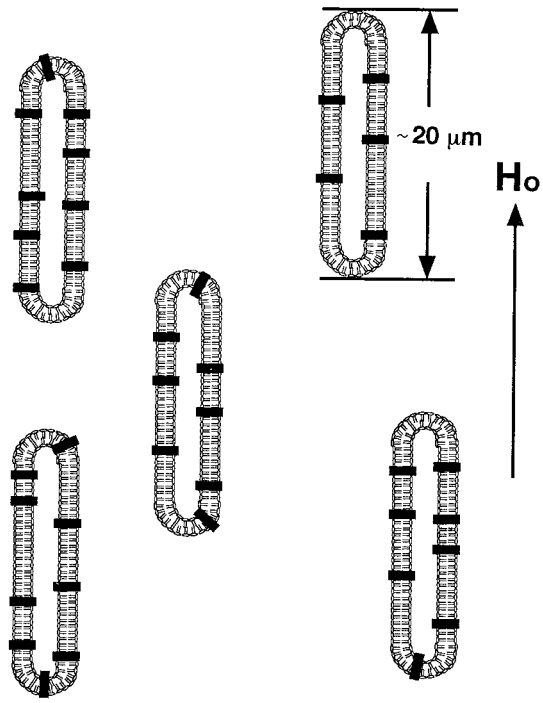

FIGURE 8 Schematic representation of the elongated vesicles of melittin-DMPC bilayers in the presence of a strong magnetic field. The longer axis is parallel to the magnetic field, and most of the bilayer surface in the vesicles is parallel to the magnetic field. The melittin molecule forms a transmembrane helix with the helical axis parallel to the bilayer normal. The average length of the longer axis is ~20 μm.

the isotropic chemical shift values of ^{13}C-labeled amino acid residues with reference to those of model systems. In particular, the isotropic chemical shifts of the carbonyl, Cα and Cβ carbons of a variety of amino acid residues are known to vary, reflecting a variety of secondary structures based on model peptides (Saitô and Ando, 1989; Saitô et al., 1998). Because the isotropic ^{13}C chemical shifts of [1-^{13}C]Gly^3, [1-^{13}C]Val^5, [1-^{13}C]Gly^{12}, [1-^{13}C]Leu^{16}, and [1-^{13}C]Ile^{20} residues in melittin are found to be 172.7, 175.2, 171.6, 175.6 and 174.8 ppm, respectively, all of the residues mentioned above are involved in the α-helix, as summarized in Table 1. Similarly, the isotropic ^{13}C chemical shift of Ala^{15} Cβ at 16.1 ppm is consistent with that of the α-helical structure (Saitô and Ando, 1989; Saitô et al., 1998). It is noticed that the Gly^3 and Val^5 residues form α-helices despite their locations at the N-terminal region, although the N- and C-termini (Gly^1-Val^5 and Arg^{22}-Gln^{26}, respectively) were shown to take on a less-oriented structure, based on a TRNOE experiment (Okada et al., 1994). Indeed, the isotropic chemical shift value (172.7 ppm) for Gly^3 is larger than the typical value for the α-helix (171.5 ppm). Furthermore, the principal values (238, 187, and 93 ppm) of the chemical shift tensor for Gly^3 in the rigid case also deviate substantially from those (240, 178, 95 ppm) of a typical α-helix of Gly residues (Ando et al., 1985). These results indicate that the α-helix around Gly^3 is substantially distorted.

Dynamics of melittin bound to DMPC bilayers based on slow MAS NMR pattern

The dynamics of melittin in DMPC bilayers can be clearly visualized in the ^{13}C NMR lineshapes recorded at various temperatures, as shown in Fig. 4. At 30°C, the lipid bilayer containing melittin is oriented with respect to the magnetic field. Nevertheless, the ^{13}C NMR spectra of Gly^3 C═O at 30°C show broad lines as compared with those at 40°C. This broadening is caused by the interference of averaging of the chemical shift anisotropy rather than residual ^{13}C-^{13}C dipolar interaction, because the motional frequency of the helix about the helical axis is near 15 kHz at 30°C. (We noticed that the linewidth (~400 Hz) for the static spectra is ~100 Hz broader than that (~300 Hz) for the MAS spectra. Because mostly singly ^{13}C-labeled melittin molecules were used for ^{13}C NMR measurements, one can expect that only the intermolecular ^{13}C-^{13}C dipolar interactions can contribute to broadening of the linewidth. However, ~100 Hz of the ^{13}C-^{13}C dipolar interaction is expected for the ^{13}C-^{13}C distance of 4 Å, even for a rigid melittin. Therefore, we conclude that the ^{13}C-^{13}C dipolar interaction is reduced to a large extent by molecular motion and can contribute a line broadening less than the linewidth of melittin bound to membrane at a temperature higher than the T_m. Instead, the disorder of orientation in melittin bound to membrane, if any, which contributes ~100 Hz of line broadening, appeared in the static NMR spectra compared with that in the MAS. Furthermore, the much larger linewidth of the C═O carbon nuclei in melittin bound to membrane, compared with that in lipid in the MAS experiments, reflects the fact that interference with the chemical shift anisotropy in melittin contributes to a large extent to the line broadening. Thus, motion of melittin is on the order of 15 kHz and is much slower than that of lipids.) At 20°C, the bilayer is not magnetically oriented, and hence the powder pattern should be observed. Although the powder pattern was observed, the linewidth of Gly^3 C═O is not as large as 15 kHz, which is the case of rigid carbonyl chemical shift anisotropy obtained at −60°C, as summarized in Table 1. Therefore, the reorientation of the helix is not completely frozen at a temperature above 20°C. It is considered that melittin forms two α-helical rods over the entire region connected around Thr^{11} and Gly^{12}, as is observed by solution NMR studies (Inagaki et al., 1989; Okada et al., 1994). In this work, the ^{13}C isotropic chemical shift values obtained from the fast MAS experiment indicate that the melittin forms α-helix, as viewed from Gly^3, Val^5, Gly^{12}, Ala^{15}, Leu^{16}, and Ile^{20} residues. It is therefore reasonable to assume that the two melittin helices reorient with a large amplitude about the helical axis in the membrane-bound state.

We now utilize the ^{13}C chemical shift tensors of the carbonyl carbon forming the α-helix to reveal the molecular motion. It has been reported that the principal directions of δ_{22} and δ_{33} are nearly parallel to the C═O bond direction and the peptide plane normal, respectively, and δ_{11} is perpendicular to both δ_{22} and δ_{33} axes (Hartzell et al., 1987), as is schematically depicted in Fig. 9. We assume that the C═O direction in an α-helix is nearly parallel to the helical axis, to form C═O···H-N hydrogen bonds (both α and β are 90° in Fig. 9). Under this condition, an axially symmetrical powder pattern characterized by $\delta_{\parallel}$ and $\delta_{\perp}$, corresponding to δ_{22} and $(\delta_{11} + \delta_{33})/2$, respectively, is obtained as shown in Fig. 9 *b*, when the helix rotates rapidly about the helical axis. We have determined that the principal values δ_{11}, δ_{22}, and δ_{33} of the chemical shift tensor of Ile^{20} C═O are 241, 189, and 96 ppm, respectively, in the low-temperature experiments. Therefore, the average ^{13}C chemical shift tensor becomes axially symmetrical to give $\delta_{\perp} = (\delta_{11} + \delta_{33})/2 = 168$ and $\delta_{\parallel} = \delta_{22} = 189$ ppm. Indeed, an axially symmetrical powder pattern with $\delta_{\perp} = 170$ and $\delta_{\parallel} = 185$ ppm was obtained for Ile^{20} C═O in the slow MAS experiment, which agrees well with the values obtained from the motional model as mentioned above. In the case of Gly^3 C═O, $\delta_{\perp} = 165$ and $\delta_{\parallel} = 187$ ppm were evaluated from the principal values ($\delta_{11} = 238$, $\delta_{22} = 187$, and $\delta_{33} = 93$ ppm) obtained from the powder pattern recorded at −60°C, whereas $\delta_{\perp} = 180$ and $\delta_{\parallel} = 159$ ppm were obtained from the slow MAS experiment as shown in Fig. 7. The axially symmetrical powder pattern for Gly^3 C═O was reversed in shape as compared to that for Ile^{20} C═O. This observation suggests that the C═O direction of Gly^3 is not parallel to

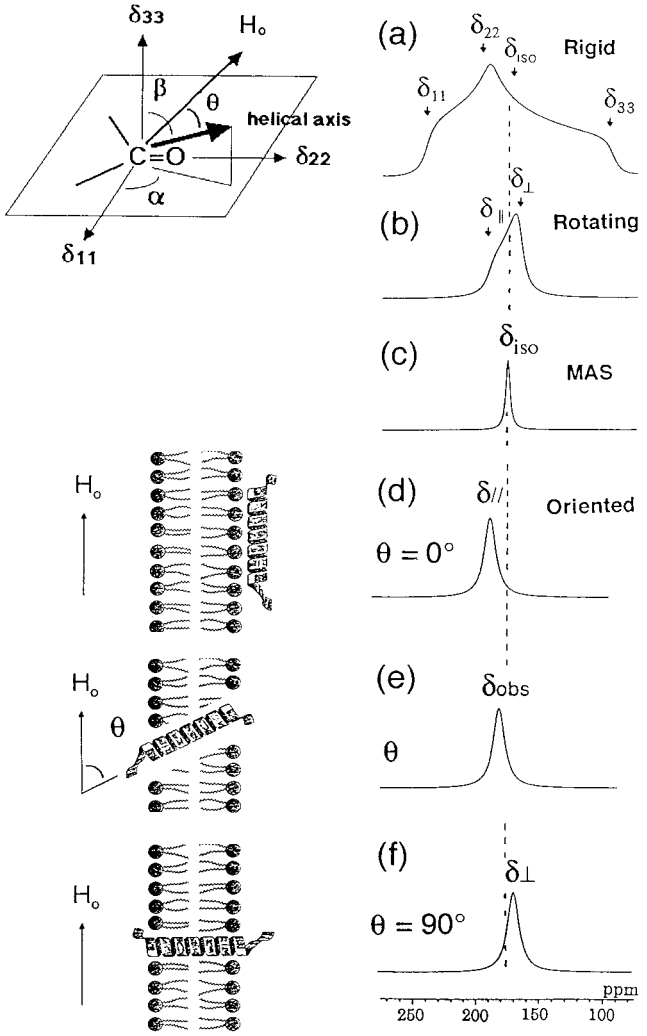

FIGURE 9 Directions of the principal axes of the ^{13}C chemical shift tensor of the C═O group, helical axis, and static magnetic field (H_o), and ^{13}C NMR spectral patterns of the C═O carbons corresponding to the orientation of the α-helix with respect to the surface of the magnetically oriented lipid bilayers. Simulated spectra were calculated using $\delta_{11} = 241$, $\delta_{22} = 189$, and $\delta_{33} = 96$ ppm (principal values of Ile[20] C═O at −60°C) for the rigid case (*a*), rotation about the helical axis (slow MAS) (*b*), fast MAS (c), magnetic orientation parallel to the magnetic field (*d*), an angle θ with the magnetic field (*e*), and the direction perpendicular to the magnetic field (*f*).

the rotation axis, as discussed later. In the case of Val[5] C═O, the anisotropy, $\Delta\delta = (\delta_{\parallel} - \delta_{\perp})$, should be found to be 23 ppm, using the δ_{11}, δ_{22}, and δ_{33} values of 238, 191, and 97 ppm, respectively, on the basis of the spectrum at −60°C (Table 1). Instead, 5.4 ppm of the $|\delta_{\parallel} - \delta_{\perp}|$ value was obtained by the slow MAS experiments (Table 1) for Val[5] C═O. In a similar manner, decreased anisotropy was observed for the Gly[12] and Leu[16] C═O carbons.

Although so far we have considered that the α-helix of melittin rotates about the helical axis in the liquid crystalline phase of lipid bilayers at a temperature above the T_m, other possibilities of motion should be taken into account to explain such a large difference in the anisotropic patterns from those evaluated using the above model for the Gly[3], Val[5], Gly[12], Leu[16], and Ile[20] C═O carbons in the slow MAS experiment. First, the local motion of helical rods is worth considering. In particular, Gly[12] may have larger mobility because it is located very close to the kink at the Pro residue, which does not form N-H···O═C hydrogen bonding. However, the kink is not very wide, and hence it is not likely to show isotropic motion in the center of the melittin helix, although it may contribute in part to reduction of the linewidth. Second, one can consider that the C═O direction largely deviates from the rapid rotating helical axis. Third, precession or reorientation about the axis other than the helical axis may average the chemical shift anisotropy. We now consider the second possibility of motion. To evaluate how the lineshape varies when the C═O direction corresponding to the δ_{22} direction deviates from the α-helical axis, we calculated the lineshape in the slow MAS experiment by assuming that the α-helix rotates rapidly about the helical axis as shown in Fig. 10. The calcu-

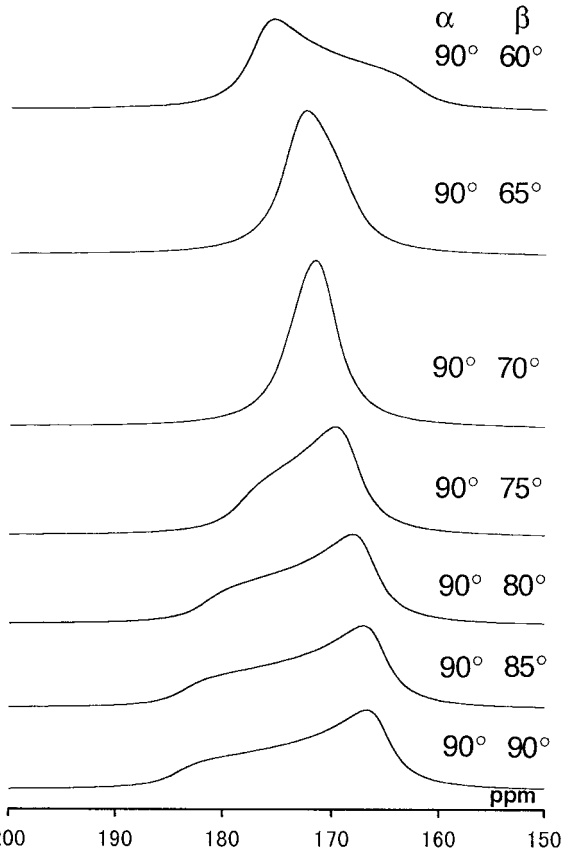

FIGURE 10 Simulated ^{13}C NMR spectra of the backbone carbonyl carbons of melittin bound to DMPC, using $\delta_{11} = 238$, $\delta_{22} = 187$, and $\delta_{33} = 93$ ppm (principal values of Gly[3] C═O at −60°C). α-Helices are rotating rapidly about the helical axis in the orientation defined by α and β, denoted as in Fig. 9.

lated results show that anisotropy of the powder pattern $|\delta_{\parallel} - \delta_{\perp}|$ is largely scaled down when the helical axis deviates from the δ_{22} toward δ_{33} direction. We also noticed that the order of $\delta_{\parallel}$ and $\delta_{\perp}$ is altered when $90° - \beta$ is larger than 25°. Actually, the lineshape for Gly^3 C═O is close to the case where the $90° - \beta$ value is 30°. This rather large angle can be expected, because Gly^3 is located nearly at the end of the N-terminal region.

As far as the rotational motion about the helical axis exists, the large reduction of the anisotropies for the Val^5, Gly^{12}, and Leu^{16} can be explained in terms of the fairly large angle between the helical axis and the δ_{22} axis toward δ_{33} axis. Indeed, the angles of 30, 20, 20, 20, and 10° were evaluated from the simulated spectra in Fig. 10 for Gly^3, Val^5, Gly^{12}, Leu^{16}, and Ile^{20}, respectively. Because the C═O axis is nearly parallel to the helical axis, which deviates by only ~12° from the peptide plane (Smith et al., 1994), it is more reasonable to assume that the helical axis of melittin is considered to precess about the average helical axis rather than the helical axis, as mentioned in the third possibility of motion. This sort of precession of the helical axis about the average helical axis clearly explains why the C═O axis is inclined largely to the δ_{33} axis. Therefore, we suggest that melittin molecules rotate rapidly about the averaged helical axis of the whole body of melittin, whose N- and C-terminal helical rods are inclined about 30° ± 12° and 10° ± 12° to the average helical axis, as estimated from the ^{13}C chemical shift values of [1-^{13}C]Gly^3-melittin and [1-^{13}C]Ile^{20}-melittin molecules, respectively. The error range was estimated by considering the possibility of the deviation of C═O axis from the helical axis by the range from 0 to 12°. The chemical shift values of [1-^{13}C]Gly^3 and [1-^{13}C]Ile^{20} were used in this discussion to determine the tilt angle, because the clear axially symmetrical powder patterns were observed for these amino acid residues. Hence the two possible kink angles between the N- and C-terminal helical axes are estimated as 140° ± 24° or 160° ± 24° (Fig. 11 *a*), which is considerably larger than 120°, as reported by an x-ray diffraction study of the static condition (Terwilliger et al., 1982). (In the crystalline state, melittin adopts a tetrameric form. The large helix bend allows optimal packing of hydrophobic side chains with the melittin tetramer. On the other hand, the large kink angle of 160° is obtained from the monomeric melittin in methanol (Bazzo et al., 1988). Obviously, it appears that a melittin structure such as a kink angle is strongly influenced by the environment. Thus the kink angle may vary within or outside the membrane, and depending on factors in the membrane environment, such as thickness and acidity of membranes. In the case of DMPC-melittin bilayers, the kink angle of melittin might be taken to be a proper angle for locating both ends of the N- and C- terminals near the polar groups on both sides of the membrane as a transmembrane helix.)

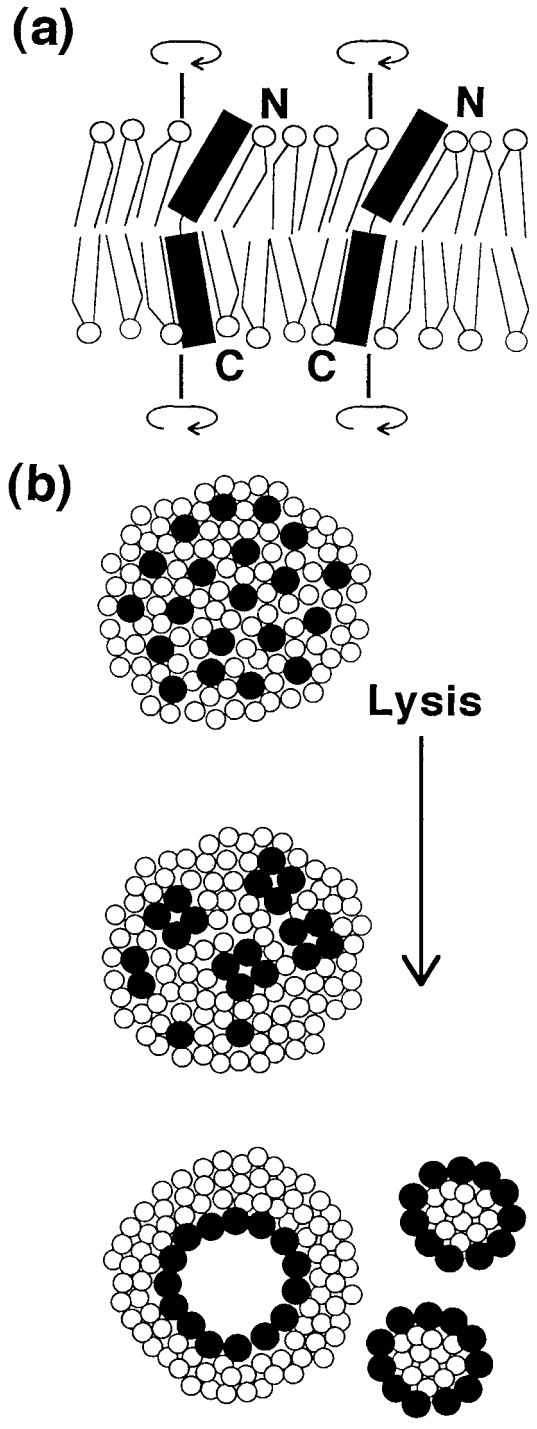

FIGURE 11 (*a*) Schematic representation of the orientation of melittin helices bound to magnetically oriented lipid bilayers. N- and C-terminal helix axes make angles of 30° and 10°, respectively, with the average axis, which is perpendicular to the bilayer surface. Two kink angles (140° and 160°) can be taken, but they cannot be distinguished by this NMR experiment. (*b*) The lytic process of lipid bilayers in the presence of melittin at temperatures below T_m. ○, ●, Lipid and melittin molecules, respectively.

Detailed analysis of orientation of melittin in DMPC bilayers based on ^{13}C NMR spectra of a magnetically oriented system

The aforementioned ^{31}P NMR signal indicates that the melittin-DMPC lipid bilayer is oriented with the bilayer surface parallel to the static magnetic field above 30°C. Therefore, because it interacts strongly with the lipid bilayer, we can evaluate how the melittin helix is oriented with respect to the lipid bilayer plane in view of the ^{13}C NMR spectra of melittin.

We now consider the $^{13}C{=}O$ chemical shift tensor to evaluate the orientation of α-helical peptides bound to the magnetically oriented lipid bilayer in a general case where the C═O axis is not parallel to the helical axis. In this case, the α-helical axis is defined as the polar angles α and β with respect to the principal axes of the $^{13}C{=}O$ chemical shift tensor, as shown in the top of Fig. 9. When the α-helix is rotated rapidly about the helical axis and the α-helical axis is inclined θ to the static magnetic field, the observed ^{13}C chemical shift value, δ_{obs}, for the rotating α-helix in the magnetically oriented state obtained from the static experiment, can be given by (Mehring, 1983)

$$\delta_{obs} = \delta_{iso} + (1/4)(3\cos^2\theta - 1)[(3\cos^2\beta - 1)(\delta_{33} - \delta_{iso}) + \sin^2\beta\cos 2\alpha(\delta_{11} - \delta_{22})]. \quad (1)$$

When $\theta = 0°$, the α-helical axis is considered to be parallel to the static magnetic field. In that direction, δ_{obs} is denoted as $\delta_{\parallel}$ and is given by

$$\delta_{/\!/} = \delta_{iso} + (1/2)[(3\cos^2\beta - 1)(\delta_{33} - \delta_{iso}) + \sin^2\beta\cos 2\alpha(\delta_{11} - \delta_{22})]. \quad (2)$$

When $\theta = 90°$, the α-helix is perpendicular to the static magnetic field, and then δ_{obs} corresponds to $\delta_{\perp}$ and is expressed as

$$\delta_{\perp} = \delta_{iso} - (1/4)[(3\cos^2\beta - 1)(\delta_{33} - \delta_{iso}) + \sin^2\beta\cos 2\alpha(\delta_{11} - \delta_{22})]. \quad (3)$$

Using the relation of Eqs. 2 and 3, Eq. 1 can be given by

$$\delta_{obs} = \delta_{iso} + (1/3)(3\cos^2\theta - 1)(\delta_{\parallel} - \delta_{\perp}). \quad (4)$$

This relation allows one to predict that the α-helix is parallel to the magnetic field when δ_{obs} is displaced downfield up to $\delta_{\parallel}$, while the α-helix is perpendicular to the magnetic field when δ_{obs} is displaced upfield up to $\delta_{\perp}$, as shown in Fig. 9, *d* and *f*, respectively, for the case where $\delta_{\parallel}$ appears at a lower field than $\delta_{\perp}$ does. Generally, the orientation of the α-helical axis with respect to the lipid bilayer surface, θ, can be determined by using Eq. 4 after δ_{iso}, δ_{obs}, and $\delta_{\parallel} - \delta_{\perp}$ values are obtained from the MAS, static, and slow MAS experiments, respectively.

Because it turned out, in the previous section, that the lipid bilayer is oriented with respect to the magnetic field with the bilayer surface parallel to the magnetic field and the α-helical axis of melittin precessed about the averaged helical axis, θ reflects the direction of the average α-helix with respect to the surface of the lipid bilayer. Actually, the static ^{13}C chemical shift (δ_{obs}) of Ile^{20} C═O in the magnetically oriented state was displaced upfield by 4.6 ppm from the isotropic value (δ_{iso}). This value allows one to determine the average α-helical axis inclined nearly 90° to the bilayer plane. On the other hand, that of Gly^3 C═O was displaced downfield by 6.8 ppm, whereas the axially symmetrical powder pattern was reversed in shape as compared to that of Ile^{20} C═O, and hence the $\delta_{\parallel} - \delta_{\perp}$ value is negative in this case. This result leads to the conclusion that the average axis of the α-helix is inclined again ~90° to the bilayer plane. We have evaluated the θ values for a variety of labeled residues as summarized in Table 1. The angle for θ in the α-helical region around Gly^3 and Val^5 is nearly 90°, indicating that the α-helical rod of the N-terminal region is inserted into the lipid bilayer parallel to the bilayer normal. Similarly, the α-helical rod of the C-terminal region is inserted into the bilayer, making an angle of ~90° with the bilayer plane, which is again parallel to the bilayer normal as calculated for Ile^{20}. Therefore, we conclude that the transmembrane α-helices of melittin are formed in the lipid bilayer systems and that both N- and C-terminal helices reorient about the average helical axis, which is parallel to the lipid bilayer normal (Fig. 11 *a*). It is emphasized that the charged amino acid residues such as Lys^7 in the N-terminus and Lys^{21}, Arg^{22}, Lys^{23}, and Arg^{24} in the C-terminus may be closely located at the opposite sides of the polar headgroups of lipid bilayers, although melittin forms the amphiphilic helix in the lipid bilayer.

Structure-lysis relationship of melittin in lipid bilayers

It is of interest to discuss the dynamic structure of melittin in a lipid bilayer in relation to its lytic activity. The present results indicate that melittin forms the transmembrane α-helix in the lipid bilayer, whose average axis is parallel to the bilayer normal. It was also shown that the transmembrane helix is not static, but undergoes motion described in the previous section, namely, the N- and C-terminal α-helical rods rotate or reorient rapidly about the average helical axis. Although the average direction of the α-helical axis is parallel to the bilayer normal, the local helical axis may precess about the bilayer normal by making an angle of 30° and 10° for the N- and C-terminal helical rods, respectively, as shown in Fig. 11 *a*. This observation is in contrast to the previously proposed conformations where the amphiphilic helix lies with its axis parallel to the bilayer surface, based on the finding that all three Lys residues in melittin are

accessible to the aqueous solvent (Altenbach et al., 1989; Stanislawski and Ruterjans, 1987). On the other hand, our observations agree with an alternative view that the melittin helix is preferentially parallel to the bilayer normal, as studied by ATR IR in the mechanically aligned bilayer (Vogel et al., 1983; Braunner et al., 1987). Smith et al. (1994) also reported that the melittin helix is oriented perpendicular to the membrane surface in which the membrane is oriented on the glass plate. However, in their system, the carbonyl ^{13}C chemical shifts of the entire region of the helical rod are displaced upfield when the mechanically aligned lipid bilayer surface is parallel to the magnetic field, indicating that the helical axis is also perpendicular to the surface of the lipid bilayer. In addition, the chemical shift anisotropies do not decrease in the central part of the helix in the lipid bilayer on the glass plate, although the rapid rotation about the helical axis undergoes averaging of the anisotropy. Moreover, the cross-polarization was effective for their system, whereas it was not in this case, indicating that the mobility and kink angle of melittin are smaller than those of our system. This discrepancy may be attributed to the different extent of hydration because the lipid bilayer vesicle used in this study is highly hydrated. Although Frey and Tamm (1991) proposed that orientation of melittin helices in membranes depends on the degree of hydration of the model membrane and the α-helix long axis of melittin is oriented parallel to the bilayer surface in the highly hydrated state, our results indicate that the transmembrane α-helix is formed even in a highly hydrated state.

It is of interest to relate the lytic activity of melittin to the molecular association in the lipid bilayer, as shown schematically in Fig. 11 *b*. Although we did not obtain detailed information on the molecular association from this NMR experiment alone, the dynamic behavior of melittin strongly suggests that it exists as monomers in the lipid bilayer at temperatures higher than T_m. When monomeric melittin adopts the transmembrane α-helical form in the lipid bilayer, we explain that lysis can be initiated by the association of melittin molecules in the lipid bilayer to separate the lipid bilayer surface, resulting in the pore formation of the lipid bilayer as observed in the microscope. After growing a number of pores, small areas of the lipid bilayer are surrounded by melittin helices to form small discoidal bilayers to disperse in the solution, as reported by Dufourcq et al. (1986). The monomeric transmembrane form of melittin is considered to be unstable in the lipid bilayers because of the amphiphilic nature of the melittin helix. These unstable helices might associate to make pores by aligning the hydrophobic side toward the lipid bilayer. This lytic activity might therefore be related to the lateral diffusion of lipid bilayers rather than the structural change of melittin, because this lytic behavior is altered at a temperature across the T_m.

CONCLUSIONS

It is clearly demonstrated that the DMPC bilayer in the presence of melittin exhibits very high magnetic ordering at a temperature above T_m by forming elongated vesicles. Because the long axis is assumed to be much longer than the short one, most of the bilayer surface is parallel to the magnetic field. This magnetically oriented bilayer is an excellent medium for investigating the relative orientation of membrane-bound peptides with respect to bilayer systems. In the case of melittin bound to this magnetically oriented lipid bilayer, the ^{13}C chemical shift anisotropy ($\delta_{\parallel} - \delta_{\perp}$) of the carbonyl carbons obtained from the slow MAS experiment indicates that melittin undergoes rotation or reorientation of the whole α-helical rod about the average helical axis rather than the helical axis. Furthermore, the ^{13}C chemical shift value (δ_{obs}) of the oriented melittin bound to the magnetically aligned bilayer system suggests that melittin forms the transmembrane α-helix and the average helical axis is aligned parallel to the bilayer normal. It was also revealed that the N- and C-terminal α-helical rods of melittin are tilted, respectively, by 30° and 10° from the bilayer normal, and the kinked angle at the central part is 140° or 160° in the lipid bilayer. The lytic activity of melittin toward the lipid bilayer can be explained in terms of spontaneous association of melittin in the lipid bilayer, resulting in the formation of pores in the lipid bilayer surface to separate the lipid bilayers and, consequently, in the complete fragmentation into disc-type micelles.

The authors thank Prof. T. Shimmen and Mr. S. Toraya of the Himeji Institute of Technology for their advice on measuring the microscopy.

This work was supported, in part, by Grants-in-Aid for Scientific Research from the Ministry of Education, Science, Culture, and Sports of Japan.

REFERENCES

Altenbach, C., W. Froncisz, J. S. Hyde, and W. L. Hubbell. 1989. Conformation of spin-labeled melittin at membrane surfaces investigated by pulse saturation recovery and continuous wave power saturation electron paramagnetic resonance. *Biophys. J.* 56:1183–1191.

Ando, S., T. Yamanobe, I. Ando, A. Shoji, T. Ozaki, R. Tabeta, and H. Saitô. 1985. Conformational characterization of glycine residues incorporated into some homopolypeptides by solid-state ^{13}C NMR spectroscopy. *J. Am. Chem. Soc.* 107:7648–7652.

Bazzo, R., M. J. Tappin, A. Pastore, T. S. Harvey, J. A. Carver, and I. D. Campbell. 1988. The structure of melittin. A ^{1}H-NMR study in methanol. *Eur. J. Biochem.* 173:139–146.

Beschiaschvili, G., and J. Seelig. 1990. Melittin binding to mixed phosphatidylglycerol/phosphatidylcholine membranes. *Biochemistry.* 29:52–58.

Brauner, J. W., R. Mendelsohn, and F. G. Prendergast. 1987. Attenuated total reflectance Fourier transform infrared studies of the interaction of melittin, two fragments of melittin, and δ-hemolysin with phosphatidylcholines. *Biochemistry.* 26:8151–8158.

Brown, L. R., J. Lauterwein, and K. Wüthrich. 1980. High-resolution ^{1}H-NMR studies of self-aggregation of melittin in aqueous solution. *Biochem. Biophys. Acta.* 622:231–244.

Brumm, T., A. Möps, C. Dolainsky, S. Brückner, and T. M. Bayerl. 1992. Macroscopic orientation effects in broadline NMR-spectra of model membranes at high magnetic field strength: a method preventing such effects. *Biophys. J.* 61:1018–1024.

Citra, M. J., and P. H. Axelsen. 1996. Determination of molecular order in supported lipid membranes by internal reflection Fourier transform infrared spectroscopy. *Biophys. J.* 71:1796–1805.

Dawson, C. R., A. F. Drake, J. Helliwell, and R. C. Hider. 1978. The interaction of bee melittin with lipid bilayer membranes. *Biochem. Biophys. Acta.* 510:75–86.

Dempsey, C. E. 1990. The actions of melittin on membranes. *Biochim. Biophys. Acta.* 1031:143–161.

Dempsey, C. E., and B. Sternberg. 1991. Reversible disc-micellization of dimyristoylphosphatidylcholine bilayers induced by melittin and [Ala-14]melittin. *Biochem. Biophys. Acta.* 1061:175–184.

Dempsey, C. E., and A. Watts. 1987. A deuterium and phosphorus-31 nuclear magnetic resonance study of the interaction of melittin with dimyristoylphosphatidylcholine bilayers and the effects of contaminating phospholipase A_2. *Biochemistry.* 26:5803–5811.

Dufourc, E. J., J. F. Faucon, G. Fourche, J. Dufourcq, T. Gulik-Krzywicki, and M. le Maire. 1986a. Reversible disc-to-vesicle transition of melittin-DPPC complexes triggered by the phospholipid acyl chain melting. *FEBS Lett.* 201:205–209.

Dufourc, E. J., I. C. P. Smith, and J. Dufourcq. 1986b. Molecular details of melittin- induced lysis of phospholipid membranes as revealed by deuterium and phosphorous NMR. *Biochemistry.* 25:6448–6455.

Dufourcq, J., J. F. Faucon, G. Fourche, J. L. Desseux, M. Le Maire, and T. Gulik- Krzywicki. 1986. Morphological changes of phosphatidylcholine bilayers induced by melittin: vesicularization, fusion, discoidal particles. *Biochem. Biophys. Acta.* 859:33–48.

Fields, G. B., Z. Tian, and G. Barany. 1992. Principle and practice of solid-phase peptide synthesis. *In* Synthetic Peptides. G. A. Grant, editor. W. H. Freeman and Company, New York. 77–184.

Frey, S., and L. K. Tamm. 1991. Orientation of melittin in phospholipid bilayers: a polarized attenuated total reflection infrared study. *Biophys. J.* 60:922–930.

Habermann, E. 1972. Bee and wasp venoms. *Science.* 177:314–322.

Habermann, E., and J. Jentsch. 1967. Sequenzanalyse des melittins aus den tryptischen und peptischen spaltstücken. *Hoppe-Seyler's Z. Physiol. Chem.* 348:37–50.

Hartzell, C. J., M. Whitfield, T. G. Oas, and G. P. Drobny. 1987. Determination of the ^{15}N and ^{13}C chemical shift tensors of L-[^{13}C]alanyl-L-[^{15}N]alanine from the dipole-coupled powder patterns. *J. Am. Chem. Soc.* 109:5966–5969.

Howard, K. P., and S. J. Opella. 1996. High-resolution solid-state NMR spectra of integral membrane proteins reconstituted into magnetically oriented phospholipid bilayers. *J. Magn. Reson.* 112B:91–94.

Inagaki, F., I. Shimada, K. Kawaguchi, M. Hirano, I. Terasawa, T. Ikura, and N. Go. 1989. Structure of melittin bound to perdeuterated dodecylphosphocholine micelles as studied by two-dimensional NMR and distance geometry calculations. *Biochemistry.* 28:5985–5991.

Kemf, C., R. D. Klausner, J. N. Weinstein, J. Van Renswoude, M. Pincus, and R. Blumenthal. 1982. Voltage-dependent trans-bilayer orientation of melittin. *J. Biol. Chem.* 257:2469–2476.

Lauterwein, J., L. R. Brown, and K. Wüthrich. 1980. High-resolution ^1H-NMR studies of monomeric melittin in aqueous solution. *Biochem. Biophys. Acta.* 622:219–230.

Mehring, M. 1983. Principles of High Resolution NMR in Solids. Springer-Verlag, Berlin.

Monette, M., and M. Lafleur. 1995. Modulation of melittin-induced lysis by surface charge density of membranes. *Biophys. J.* 68:187–195.

Morgan, C. G., H. Williamson, S. Fuller, and B. Hadson. 1983. Melittin induces fusion of unilamellar phospholipid vesicles. *Biochim. Biophys. Acta.* 732:668–674.

Okada, A., K. Wakamatsu, T. Miyazawa, and T. Higashijima. 1994. Vesicle-bound conformation of melittin: transferred nuclear Overhauser enhancement analysis in the presence of perdeuterated phosphatidylcholine vesicles. *Biochemistry.* 33:9438–9446.

Paquet, A. 1982. Introduction of 9-fluorenylmethyloxycarbonyl, trichloroethoxycarbonyl, and benzyloxycarbonyl amine protecting group into O-unprotected hydroxyamino acids using succinimidyl carbonates. *Can. J. Chem.* 60:976–980.

Pott, T., and E. J. Dufourc. 1995. Action of melittin on the DPPC-cholesterol lipid- ordered phase: a solid state ^2H- and ^{31}P-NMR study. *Biophys. J.* 68:965–977.

Prosser, R. S., S. A. Hunt, J. A. DiNatale, and R. R. Vold. 1996. Magnetically aligned membrane model systems with positive order parameter: switching the sign of S_{zz} with paramagnetic ions. *J. Am. Chem. Soc.* 118:269–270.

Qiu, X., P. A. Mirau, and C. Pidgeon. 1993. Magnetically induced orientation of phosphatidylcholine membranes. *Biochim. Biophys. Acta.* 1147:59–72.

Saitô, H., and I. Ando. 1989. High-resolution solid-state NMR studies of synthetic and biological macromolecules. *Annu. Rep. NMR Spectrosc.* 21:209–290.

Saitô, H., S. Tuzi, and A. Naito. 1998. Empirical versus non-empirical evaluation of secondary structure of fibrous and membrane proteins by solid-state NMR: a practical approach. *Annu. Rep. NMR Spectrosc.* 36:79–121.

Sanders, C. R. 1993. Solid state ^{13}C NMR of unlabeled phosphatidylcholine bilayers: spectral assignments and measurement of carbon-phosphorus dipolar couplings and ^{13}C chemical shift anisotropies. *Biophys. J.* 64:171–181.

Sanders, C. R., and J. H. Prestegard. 1990. Magnetically orientable phospholipid bilayers containing small amount of a bile salt analogue, CHAPSO. *Biophys. J.* 58:447–460.

Sanders, C. R., and J. P. Schwonek. 1992. Characterization of magnetically orientable bilayers in mixtures of dihexanoylphosphatidylcholine and dimyristoylphosphatidylcholine by solid-state NMR. *Biochemistry.* 31: 8898–8905.

Scholz, F., E. Boroske, and W. Helfrich. 1984. Magnetic anisotropy of lecithin membranes: a new anisotropy susceptometer. *Biophys. J.* 45: 589–592.

Seelig, J., F. Borle, and T. A. Cross. 1985. Magnetic ordering of phospholipid membranes. *Biochim. Biophys. Acta.* 814:195–198.

Sessa, G., J. H. Freer, G. Colacicco, and G. Weissmann. 1969. Interaction of a lytic polypeptide, melittin, with lipid membrane systems. *J. Biol. Chem.* 244:3575–3582.

Smith, I. C. P., and I. H. Ekiel. 1984. Phosphorus-31 NMR of phospholipids in membranes. *In* Phosphorous-31 NMR: Principles and Applications. D. G. Gorenstein, editor. Academic Press, Orlando, FL. 447–475.

Smith, R., F. Separovic, T. J. Milne, A. Whittaker, F. M. Bennett, B. A. Cornell, and A. Makriyannis. 1994. Structure and orientation of the pore-forming peptide, melittin, in lipid bilayers. *J. Mol. Biol.* 241: 456–466.

Speyer, J. B., P. K. Sripada, S. K. Das Gupta, G. G. Shipley, and R. G. Griffin. 1987. Magnetic orientation of sphingomyelin-lecithin bilayers. *Biophys. J.* 51:687–691.

Stanislawski, B., and H. Rüterjans. 1987. ^{13}C-NMR investigation of the insertion of the bee venom melittin into lecithin vesicles. *Eur. Biophys. J.* 15:1–12.

Talbot, J. C., J. Dufourcq, J. De Bony, J. F. Faucon, and C. Lussan. 1979. Conformational change and self association of monomeric melittin. *FEBS Lett.* 102:191–193.

Terwilliger, T. C., and D. Eisenberg. 1982. The structure of melittin. *J. Biol. Chem.* 257:6010–6015.

Terwilliger, T. C., L. Weissman, and D. Eisenberg. 1982. The structure of melittin in the form I crystals and its implication for melittin's lytic and surface activities. *Biophys. J.* 37:353–361.

Tosteson, M. T., and D. C. Tosteson. 1981. Melittin forms channels in lipid bilayers. *Biophys. J.* 36:109–116.

Vogel, H., F. Jähnig, V. Hoffmann, and J. Stümpel. 1983. The orientation of melittin in lipid membranes. A polarized infrared spectroscopy study. *Biochim. Biophys. Acta.* 733:201–209.

Worcester, D. L. 1978. Structural origins of diamagnetic anisotropy in proteins. *Proc. Natl. Acad. Sci. USA.* 75:5475–5477.